Adaptive Robust Precision Motion Control of High-Speed Linear Motors with On-line Cogging Force Compensations

Bin Yao, Chuxiong Hu and Qingfeng Wang

Abstract— **This paper studies the precision motion control of high-speed/acceleration linear motors in a commercial gantry which are subject to significant nonlinear cogging forces. A discontinuous projection based desired compensation adaptive robust controller (ARC) is constructed and implemented. Design models consisting of known basis functions with unknown weights are used to approximate various unknown nonlinear forces with model approximation errors being explicitly accounted for in the controller design process. On-line parameter adaptation is then utilized to reduce the effect of various parametric uncertainties while certain robust control laws are synthesized to effectively handle various modeling uncertainties for a guaranteed robust performance. Comparative experimental results obtained on an Anorad commercial gantry with a linear encoder resolution of 0.5 μm and a position measurement resolution of 20 nanometers by external laser interferometers are presented to illustrate the achievable control performance of the proposed control strategy in implementation. Experiments are also performed to explicitly identify the cogging forces via external force sensors. Various comparative experimental results with and without the proposed cogging force compensations are then obtained to validate the effectiveness of the approach in practical applications.**

Index Terms— **Motion Control, Linear Motor, Adaptive Robust Control**

I. Introduction

Significant efforts have been devoted to solving the difficulties in controlling linear motors [1], [6], [4], [3], [7]. In [14], the idea of adaptive robust control (ARC) [12], [13], [10] is generalized to provide a rigorous theoretic framework for the precision motion control of linear motors. In [9], the proposed ARC algorithm [14] is tested on an *epoxy* core linear motor. To reduce the effect of velocity measurement noise, a desired compensation ARC algorithm in which the regressor is calculated by reference trajectory information [11] is also presented and implemented.

In this paper, the proposed desired compensation ARC (DCARC) [9] will be extended to the control of high-speed linear motors with significant nonlinear cogging forces. For these types of linear motor, to have a smooth motion, it is necessary to explicitly compensate for the nonlinear cogging forces, which is the focus of the paper. As an alternative to feedforaward force ripple compensation [3] or feedback compensation using measurements of back EMF [5], which may demand time-consuming and costly rigorous off-line identification, one can reduce the effect of ripple forces by utilizing the particular physical structure of the ripple forces. Specifically, design models consisting of known basis functions with unknown weights are used to approximate the unknown ripple forces with on-line parameter adaptation to reduce the effect of various parametric uncertainties. Certain robust control laws are also constructed to effectively deal with various modeling uncertainties for a guaranteed robust performance.

The proposed control strategy has been partially tested on an iron core linear motor in one of the first author's previous conference papers [8]. However, the linear encoder resolution of $1\mu m$ and the maximum speed around $1m/sec$ of the iron core linear motor in [8] significantly limited its usefulness as an experimental testbed for high-speed/acceleration motions or slow motion with sub-micrometer positioning accuracy with cogging force compensation. To address this problem, a two-axes commercial high-speed gantry driven by iron-core linear motors with built-in linear encoders has recently been set-up at Zhejiang University, which will be used as the testbed for the proposed control strategy. The built-in linear encoder has a position measurement resolution of $0.5\mu m$ and a speed limit of $3m/sec$, which enables us to perform high-speed/acceleration motion tests with acceleration more than 45 m/sec^2 and velocity of 2 m/sec. To further improve the position measurement resolution, a high-precision laser interferometer feedback system with a resolution of $20nm$ is integrated into the testbed as well. Comparative experimental results for both the high-speed/acceleration motions and the slow motions are presented to illustrate the proposed method. In addition, explicitly measurements of cogging forces via external force sensors are also performed to validate the effectiveness of the proposed cogging force compensation in practical applications.

II. Dynamic Models and Problem Formulation

The system considered here is a a current-controlled three-phase iron core linear motor driving a linear positioning stage supported by recirculating bearings. In the derivation of the model, the electrical dynamics is neglected due to the much faster electric response. The mathematical model of the system can then be described by

$$M\ddot{x} = u - F, \quad F = F_f + F_r - F_d, \tag{1}$$

The work is supported in part by the US National Science Foundation (Grant No. CMS-0600516) and in part by the National Natural Science Foundation of China (NSFC) under the Joint Research Fund for Overseas Chinese Young Scholars (Grant No. 50528505).

Bin Yao is a Professor of School of Mechanical Engineering, Purdue University, West Lafayette, IN 47907, USA (byao@purdue.edu). He is also a Kuang-piu Professor and a Responsible Scientist of Mechatronic Systems Innovation Platform at the State Key Laboratory of Fluid Power Transmission and Control of Zhejiang University

Chuxiong Hu (a graduate student) and Qingfeng Wang (a professor) are with the State Key Laboratory of Fluid Power Transmission and Control, Zhejiang University, Hangzhou, China.

1-4244-1264-1/07/$25.00 ©2007 IEEE

where x represents the position of the inertia load, M is the normalized[1] mass of the inertia load plus the coil assembly, u is the input voltage to the motor, F is the normalized lumped effect of uncertain nonlinearities such as friction force F_f, cogging force F_r and external disturbance F_d (e.g. cutting force in machining). While there have been many friction models proposed [2], a simple and often adequate approach is to regard friction force as a static nonlinear function of the velocity, i.e., $F_f(\dot{x})$, which is given by

$$F_f(\dot{x}) = B\dot{x} + F_{fn}(\dot{x}), \tag{2}$$

where B is an equivalent viscous friction coefficient of the system and F_{fn} is the nonlinear Coulomb friction term which can include the Stribeck effect [2]. In practice, due to the inaccuracy of the positioning stage and ball bearings, the friction force may also depend on position x. This phenomenon is still captured by (1), since the bounded variation of position-dependent friction can be lumped into the external disturbance F_d.

Let $y_d(t)$ be the reference motion trajectory, which is assumed to be known, bounded with bounded derivatives up to the second order. The objective is to synthesize a control input u such that the output $y = x$ tracks $y_d(t)$ as closely as possible in spite of various model uncertainties.

III. Adaptive Robust Control of Linear Motor Systems

A. Design Models and Assumptions

In this paper, it is assumed that the permanent magnets of the same linear motor are all identical and are equally spaced at a pitch of P. Thus, F_r is a periodic function of position x with a period of P, i.e., $F_r(x+P) = F_r(x)$, and it can be approximated quite accurately by the first several harmonic functions of the position, which is denoted as $\bar{F}_r(x)$ and represented by

$$\bar{F}_r(x) = A_r^T S_r(x) \tag{3}$$

where $A_r = [A_{r1s}, A_{r1c}, \ldots, A_{rqs}, A_{rqc}]^T \in R^{2q}$ is the vector of unknown weights, $S_r(x) = [\sin(\frac{2\pi}{P}x), \cos(\frac{2\pi}{P}x), \ldots, \sin(\frac{2\pi q}{P}x), \cos(\frac{2\pi q}{P}x)]^T$ is the vector of known basis shape functions, and q is the numbers of harmonics used to approximate $F_r(x)$. The larger q is, the better $\bar{F}_r(x)$ approximates $F_r(x)$, but the larger number of parameters to be adapted. So a trade-off has to be made based on the particular structure of a motor. For example, in [3], it was experimentally observed that the first, the third, and the fifth harmonics are the main harmonics in the force ripple waveform.

The same as in [11], [9], a simple *continuous* static friction model is used to approximate the actual Coulomb friction $F_{fn}(\dot{x})$ in (2) for model compensation; the model used in the paper is given by $\bar{F}_{fn} = A_f S_f(\dot{x})$, where the amplitude A_f is unknown and $S_f(\dot{x})$ is a continuous shape function. With these cogging force and Coulomb friction models, the linear motor dynamics (1) can be rewritten as:

$$M\ddot{x} = u - B\dot{x} - A_f S_f(\dot{x}) - A_r^T S_r(x) + d, \tag{4}$$

where $d = (\bar{F}_{fn} - F_{fn}) + (\bar{F}_r - F_r) + F_d$.

In general, the system is subjected to parametric uncertainties due to the variations of M, B, A_f, A_r and the nominal value of the lumped disturbance d, d_n. Thus, define the unknown parameter set $\theta = [\theta_1, \theta_2, \theta_3, \theta_{4b}^T, \theta_5]^T \in \mathbf{R}^{4+2q}$ as $\theta_1 = M$, $\theta_2 = B$, $\theta_3 = A_f$, $\theta_{4b} = A_r \in \mathbf{R}^{2q}$ and $\theta_5 = d_n$. Letting the two state variables x_1 and x_2 be the position and velocity respectively, the state space representation of (4) can thus be linearly parameterized in terms of θ as

$$\dot{x}_1 = x_2, \tag{5}$$

$$\theta_1 \dot{x}_2 = u - \theta_2 x_2 - \theta_3 S_f - \theta_{4b}^T S_r(x_1) + \theta_5 + \tilde{d}, \tag{6}$$

where $\tilde{d} = d - d_n$. The following practical assumption is made

Assumption 1: The extent of the parametric uncertainties and uncertain nonlinearities are known, i.e.,

$$\theta \in \Omega_\theta \triangleq \{\ \theta :\ \ \theta_{min} < \theta < \theta_{max}\ \} \tag{7}$$

$$\tilde{d} \in \Omega_d \triangleq \{\ \tilde{d} :\ \ |\tilde{d}| \le \delta_d\ \} \tag{8}$$

where $\theta_{min} = [\theta_{1min}, \cdots, \theta_{5min}]^T$, $\theta_{max} = [\theta_{1max}, \cdots, \theta_{5max}]^T$, and δ_d are known. ◇

B. Notations and Discontinuous Projection

Let $\hat{\theta}$ denote the estimate of θ and $\tilde{\theta}$ the estimation error (i.e., $\tilde{\theta} = \hat{\theta} - \theta$). In view of (7), the following discontinuous projection type adaptation law will be used

$$\dot{\hat{\theta}} = Proj_{\hat{\theta}}(\Gamma\tau) \tag{9}$$

where $\Gamma > 0$ is a diagonal matrix, τ is an adaptation function to be synthesized later. The projection mapping $Proj_{\hat{\theta}}(\bullet) = [Proj_{\hat{\theta}_1}(\bullet_1), \cdots, Proj_{\hat{\theta}_5}(\bullet_5)]^T$ is defined in element as

$$Proj_{\hat{\theta}_i}(\bullet_i) = \begin{cases} 0 & \text{if } \hat{\theta}_i = \theta_{imax} \text{ and } \bullet_i > 0 \\ 0 & \text{if } \hat{\theta}_i = \theta_{imin} \text{ and } \bullet_i < 0 \\ \bullet_i & \text{otherwise} \end{cases} \tag{10}$$

C. ARC Controller Design

Define a switching-function-like quantity as

$$p = \dot{e} + k_1 e = x_2 - x_{2eq}, \qquad x_{2eq} \triangleq \dot{y}_d - k_1 e, \tag{11}$$

where $e = y - y_d(t)$ is the output tracking error, $y_d(t)$ is the desired trajectory to be tracked by y, and k_1 is any positive feedback gain. If p is small or converges to zero exponentially, then the output tracking error e will be small or converge to zero exponentially since $G_p(s) = \frac{e(s)}{p(s)} = \frac{1}{s+k_1}$ is a stable transfer function. So the rest of the design is to make p as small as possible. Differentiating (11) and noting (6), one obtains

$$\begin{aligned} M\dot{p} &= u - \theta_1 \dot{x}_{2eq} - \theta_2 x_2 - \theta_3 S_f - \theta_{4b}^T S_r + \theta_5 + \tilde{d}, \\ &= u + \varphi^T \theta + \tilde{d} \end{aligned} \tag{12}$$

[1]Normalized with respect to the unit of input voltage.

1-4244-1264-1/07/$25.00 ©2007 IEEE

where $\dot{x}_{2eq} \triangleq \ddot{y}_d - k_1\dot{e}$ and $\varphi^T = [-\dot{x}_{2eq}, -x_2, -S_f(x_2), -S_r(x_1), 1]$. The following ARC control law is proposed:

$$u = u_a + u_s, \qquad u_a = -\varphi^T\hat{\theta}, \tag{13}$$

where u_a is the adjustable model compensation needed for achieving perfect tracking, and u_s is a robust control law to be synthesized later. Substituting (13) into (12), and then simplifying the resulting expression, one obtains

$$M\dot{p} = u_s - \varphi^T\tilde{\theta} + \tilde{d}. \tag{14}$$

The robust control function u_s consists of two terms given by:

$$u_s = u_{s1} + u_{s2}, \quad u_{s1} = -k_{s1}p, \quad u_{s2} = -k_{s2}p, \tag{15}$$

where u_{s1} is a simple proportional feedback to stabilize the nominal system and u_{s2} is a robust feedback used to attenuate the effect of model uncertainties with a nonlinear feedback gain k_{s2}. To achieve a guaranteed robust performance, k_{s2} should be chosen large enough such that [10], [13]

$$p\{u_{s2} - \varphi^T\tilde{\theta} + \tilde{d}\} \le \varepsilon \tag{16}$$

where ε is a design parameter which can be arbitrarily small. Essentially, (16) shows that u_{s2} is synthesized to dominate the model uncertainties coming from both parametric uncertainties $\tilde{\theta}$ and uncertain nonlinearities $\tilde{d}$ with a guaranteed attenuation level specified by ε.

Theorem 1: If the adaptation function in (9) is chosen as

$$\tau = \varphi p, \tag{17}$$

then the ARC control law (13) guarantees that [14].

A. In general, all signals are bounded. Furthermore, the positive definite function V_s defined by

$$V_s = \frac{1}{2}Mp^2 \tag{18}$$

is bounded above by

$$V_s \le \exp(-\lambda t)V_s(0) + \frac{\varepsilon}{\lambda}[1 - \exp(-\lambda t)], \tag{19}$$

where $\lambda = 2k_2/\theta_{1max}$.

B. If after a finite time t_0, there exist parametric uncertainties only (i.e., $\tilde{d} = 0$, $\forall t \ge t_0$), then, in addition to results in A, zero final tracking error is also achieved, i.e, $e \longrightarrow 0$ and $p \longrightarrow 0$ as $t \longrightarrow \infty$.

IV. Desired Compensation ARC

In the ARC design presented in Section 3, the regressor φ in the model compensation u_a (13) and adaptation function τ (17) depend on states x_1 and x_2. Such an adaptation structure may be sensitive to measurement noise and consequently, a slow adaptation rate may have to be used in implementation, which in turn reduces the effect of parameter adaptation [11]. To overcome these problems, in the following, a desired compensation ARC algorithm will be developed.

The proposed desired compensation ARC law and the adaptation function have the same form as (13) and (17) respectively, but with regressor φ substituted by the desired regressor φ_d:

$$\begin{array}{rcl} u & = & u_a + u_s, \quad u_a = -\varphi_d^T\hat{\theta}, \\ \tau & = & \varphi_d p, \end{array} \tag{20}$$

where $\varphi_d^T = [-\ddot{y}_d, -\dot{y}_d, -S_f(\dot{y}_d), -S_r(y_d), 1]$. Substituting (20) into (12), and noting $x_2 = \dot{y}_d + \dot{e}$, one obtains

$$M\dot{p} = u_s - \varphi_d^T\tilde{\theta} + \underbrace{(\theta_1 k_1 - \theta_2)\dot{e} + \theta_3[S_f(\dot{y}_d) - S_f(x_2)]}_{+\theta_{4b}^T[S_r(y_d) - S_r(x_1)]} + \tilde{d}. \tag{21}$$

Comparing (21) with (14), it can be seen that three additional terms (underbraced) appear, which may demand a strengthened robust control function u_s for a robust performance. Applying Mean Value Theorem, we have

$$\begin{array}{rcl} S_f(x_2) - S_f(\dot{y}_d) & = & g_f(x_2,t)\dot{e}, \\ S_r(x_1) - S_r(y_d) & = & g_r(x_1,t)e, \end{array} \tag{22}$$

where $g_f(x_2,t)$ and $g_r(x_1,t)$ are certain nonlinear functions. The strengthened robust control function u_s has the same form as (15):

$$u_s = u_{s1} + u_{s2}, \quad u_{s1} = -k_{s1}p, \quad u_{s1} = -k_{s2}p \tag{23}$$

but with k_{s1} being a nonlinear gain large enough such that the matrix A defined below is positive definite

$$A = \begin{bmatrix} k_{s1} - k_2 - \theta_1 k_1 + \theta_2 + \theta_3 g_f & -\frac{1}{2}(k_1\theta_2 + k_1\theta_3 g_f - \theta_{4b}^T g_r) \\ -\frac{1}{2}(k_1\theta_2 + k_1\theta_3 g_f - \theta_{4b}^T g_r) & \frac{1}{2}Mk_1^3 \end{bmatrix} \tag{24}$$

and k_{s2} is required to be large enough satisfy the following constraints similar to (16),

$$p\{u_{s2} - \varphi_d^T\tilde{\theta} + \tilde{d}\} \le \varepsilon \tag{25}$$

Theorem 2: If the DCARC law (20) is applied, then

A. In general, all signals are bounded. Furthermore, the positive definite function V_s defined by

$$V_s = \frac{1}{2}Mp^2 + \frac{1}{2}Mk_1^2e^2 \tag{26}$$

is bounded above by

$$V_s \le \exp(-\lambda t)V_s(0) + \frac{\varepsilon}{\lambda}[1 - \exp(-\lambda t)], \tag{27}$$

where $\lambda = \min\{2k_2/\theta_{1max}, k_1\}$.

B. If after a finite time t_0, there exist parametric uncertainties only (i.e., $\tilde{d} = 0$, $\forall t \ge t_0$), then, in addition to results in A, zero final tracking error is also achieved, i.e, $e \longrightarrow 0$ and $p \longrightarrow 0$ as $t \longrightarrow \infty$.

The proof of the theorem is omitted due to space limit and can be worked out similar to [9].

V. Experimental Results

A. Experimental Setup

A Precision Mechatronics Laboratory has been established at Zhejiang University, which includes a two-axes commercial Anorad HERC-510-510-AA1-B-CC2 Gantry by Rockwell Automation as shown in Fig.1. The gantry has two built-in linear encoders providing each axis a position measurement resolution of $0.5\mu m$ and a speed measurement

1-4244-1264-1/07/$25.00 ©2007 IEEE

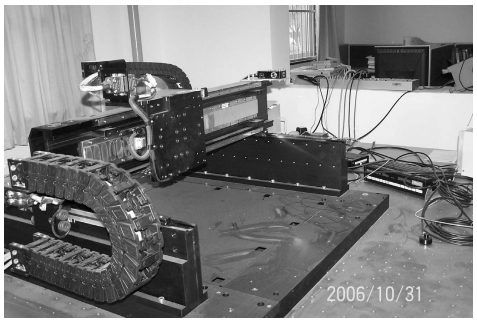

Fig. 1. Gantry Type Linear Motor Drive System

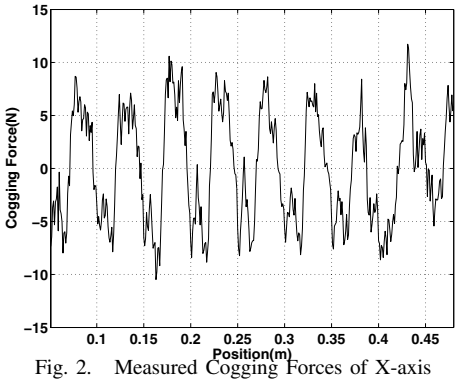

Fig. 2. Measured Cogging Forces of X-axis

limit of $3m/sec$, which will be used as the motion system hardware for this study. Both axes of the gantry are powered by Anorad LC-50-200 iron core linear motors and have a travel distance of 0.51 m. To further improve the position measurement resolution, a Renishaw RLE10-SX-XC laser position measurement system with a laser encoder compensation kit RCU10-11ABZ is used as well. The external laser interferometer system provides a direct measurement of load position with a resolution of $20nm$. The entire system is controlled through a dSPACE DS1103 controller board.

B. System Identification

Experiments have been conducted on the upper X-axis and verified the position measurement agreement of the linear encoder and the laser interferometer and their resolutions. When the power amplifier for the axis is turned on, the load carriage has a vibration amplitude around $1\mu m$ at zero input control voltage, revealing some imperfections on the electrical sub-system. Off-line parameter identification is then carried out and it is found that the nominal values are $M = 0.12volt/m/sec^2$, $B = 0.166volt/m/sec$, and $A_f = 0.15volt$.

Explicit measurement of cogging force is then conducted at various positions by blocking the motor and using an external force sensor to measurement the blocking forces at several input voltages ($0V$, $\pm 0.2V$). The backed-out cogging forces are shown in Fig. 2, which is largely a periodic function of position with the fundamental period corresponds to the pitch of the magnets ($P = 50mm$) and an amplitude around 10N. For this initial study, the first three harmonics will be compensated. Thus the basis functions are chosen as $S_r(x_1) = [\sin(\frac{2\pi}{P}x_1), \cos(\frac{2\pi}{P}x_1), \sin(\frac{4\pi}{P}x_1), \cos(\frac{4\pi}{P}x_1), \sin(\frac{6\pi}{P}x_1), \cos(\frac{6\pi}{P}x_1)]^T$.

C. Comparative Experimental Results

The control system is implemented using a dSPACE DS1103 controller board. The controller executes programs at a sampling frequency $f_s = 5kHz$, which results in a velocity measurement resolution of 0.0025 m/sec for the linear encoder feedback and 0.0001 m/sec for the laser interferometer feedback. The bounds of the parameter variations are chosen as: $\theta_{min} = [0.1, 0.15, 0.1, -0.1, -0.1, -0.1, -0.1, -0.1, -0.1, -0.5]^T$ and $\theta_{max} = [0.20, 0.35, 0.3, +0.1, +0.1, +0.1, +0.1, +0.1, +0.1, +0.5]^T$.

In [9], experimental results have shown that DCARC achieves better performance than ARC does in terms of all performance indexes. Thus in this paper, only DCARC algorithm is implemented and focus is on the comparison of the following two controllers:

DCARC1 (with cogging force compensation): the controller proposed in section 4. The robust control term u_s in (20) is implemented by simply choosing a large enough constant $k_s = k_{s1} + k_{s2}$. The parameters of the controller are chosen as: $k_1 = 400$, $k_s = 600$. The continuous function $S_f(x_2)$ is chosen as $\frac{2}{\pi}\arctan(1000x_2)$. The adaptation rates are set as $\Gamma = \mathbf{diag}\{1, 10, 100, 200, 200, 200, 200, 200, 200, 2000\}$. The initial parameter estimates are chosen as: $\hat{\theta}(0) = [0.12, 0.166, 0.1, 0, 0, 0, 0, 0, 0, 0]^T$.

DCARC2 (without cogging force compensation): The same control law as the above DCARC but without force ripple compensation, i.e., letting $\Gamma = \mathbf{diag}\{1, 10, 100, 0, 0, 0, 0, 0, 0, 2000\}$.

D. High-speed/acceleration Motion

The desired trajectory is a point-to-point movement, typical in manufacture industry, with a distance of $0.4m$, a maximum velocity of $2m/sec$ and a maximum acceleration of $45m/sec^2$. With such a high-speed and acceleration, the laser interferometer cannot be used for the position measurement. So the linear encoder of the gantry system is used for position feedback.

Fig. 3 shows the tracking error and control input for DCARC with cogging force compensation. The blow-out portions of the tracking errors for the constant speed part of the two controllers are shown in Fig. 4. As can be seen from the plots, the steady state position tracking errors of both DCARCs are within the linear encoder resolution of 0.5 μm when the system comes to a stop and mostly within 5 μm during the 2 m/sec constant speed period. Furthermore, the maximal position tracking errors during the entire motion are mostly within 20 μm. These results demonstrate the excellent tracking performance of the proposed DCARC for high-speed motions. Fig. 4 also shows the reduced low

1-4244-1264-1/07/$25.00 ©2007 IEEE

frequency content of the tracking errors when the cogging force compensation is used. The not much reduced tracking error with the cogging force compensation is due to the high closed-loop bandwidth that the proposed DCARC is able to achieve. In fact, though not shown due to space limit, when we deliberately de-tune the achievable closed-loop bandwidth, the effect of adding on-line cogging force compensation becomes rather significant.

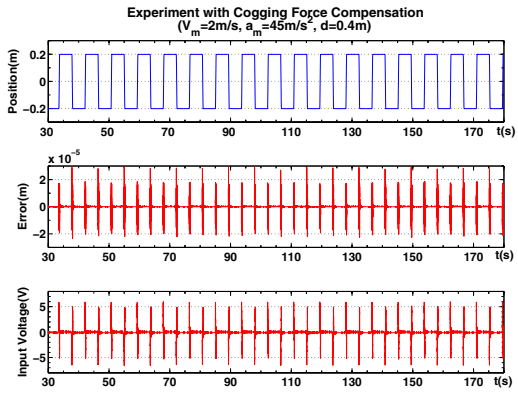

Fig. 3. High-speed/acceleration Experiment with Cogging Compensation

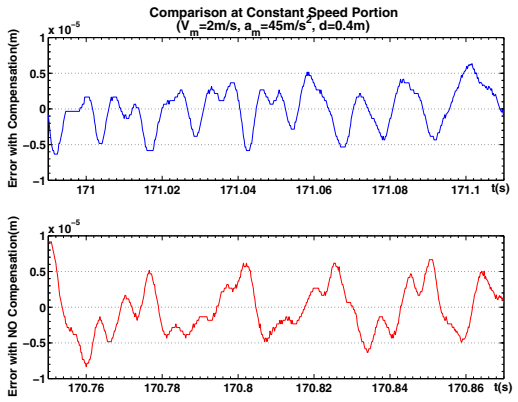

Fig. 4. High-speed/acceleration Experiment (Constant Speed Portion)

Experiments are also performed for a point-to-point movement with a distance of $0.4m$, a maximum velocity of $1m/sec$ and a maximum acceleration of $14m/sec^2$. Fig. 5 shows the tracking error and control input for DCARC with cogging force compensation. The blow-out portions of the tracking errors for the constant speed part of the two controllers are shown in Fig. 6. As can be seen from the plots, the steady state position tracking errors of both DCARCs are within the linear encoder resolution of 0.5 μm when the system comes to a stop and mostly within 5 μm during the 1 m/sec constant speed period. Furthermore, the maximal position tracking errors during the entire motion are mostly within 10 μm. These results again demonstrate the excellent tracking performance of the proposed DCARC for high-speed motions. It is seen from Fig. 6 that there is a noticeable reduction of tracking errors when the cogging force compensation is used in this case.

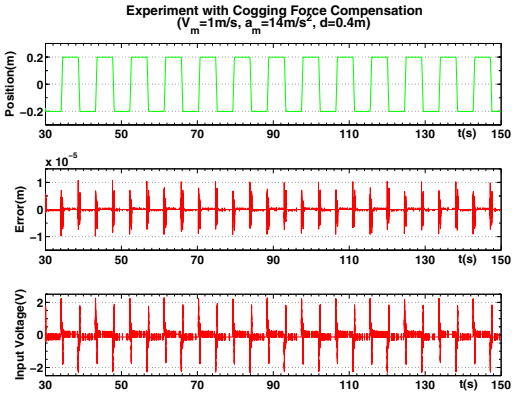

Fig. 5. High-speed/acceleration Experiment with Cogging Compensation

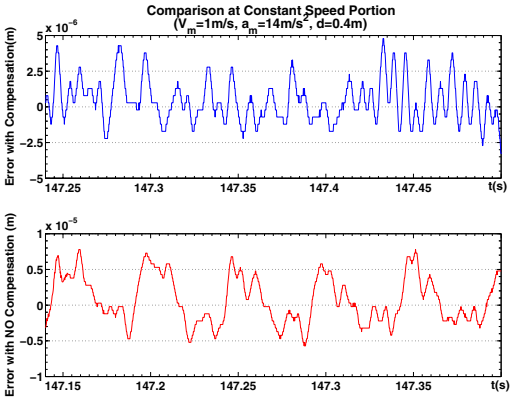

Fig. 6. High-speed/acceleration Experiment (Constant Speed Portion)

E. Low-speed Motion

The desired trajectories are the same point-to-point type movement, but with very small constant speeds of $0.02m/sec, 0.002m/sec, 0.0002m/sec$ respectively. The maximum acceleration is set at $0.5m/sec^2$, $0.05m/sec^2$, and $0.005m/sec^2$, and the travel distance is $0.1m$, $0.01m$, and $0.001m$ respectively. The $0.0002m/sec$ motion is also repeated with the velocity feedback being the average of previous 4 numerical value to reduce velocity feedback noise. For these low speed movement, the laser interferometer is used for the position measurement. In the following, only the DCARC with cogging force compensation results are shown due to the space limit.

Fig. 7 shows the tracking errors of all four experiments with the blow-out portions for the constant speed part shown in Fig. 8 and the come to stop part in Fig. 9. As can be seen from the plots, the steady-state position tracking errors are mostly within 100 nm when the system comes to a stop and within 200 nm during the constant low speed period, and the maximal position tracking error during the entire motion is within $2\mu m$. These results demonstrate the good tracking performance of the proposed DCARC for low-speed motions as well.

VI. Conclusions

In this paper, a desired compensation ARC controller with on-line cogging force compensation has been developed for

1-4244-1264-1/07/$25.00 ©2007 IEEE

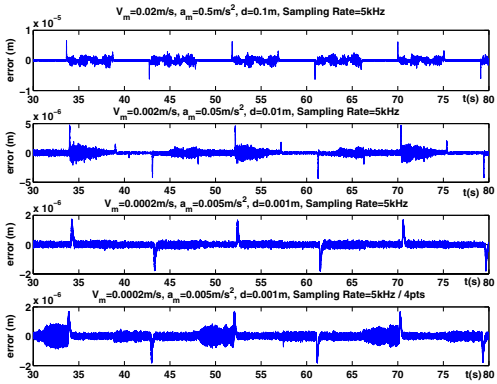

Fig. 7. Low Speed Experiments

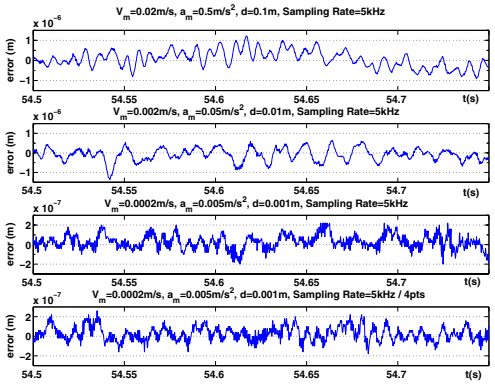

Fig. 8. Low Speed Experiments (Constant Speed Portion)

high performance robust motion control of iron core linear motors. The proposed controller takes into account the effect of model uncertainties coming from the inertia load, friction force, cogging force, and external disturbances. In particular, based on the special structure of the cogging forces, design models consisting of known basis functions with unknown weights are used to approximate the unknown nonlinear ripple forces. On-line parameter adaptation is then utilized to reduce the effect of various parametric uncertainties while the uncompensated uncertain nonlinearities are handled effectively via certain robust control laws for high performance.

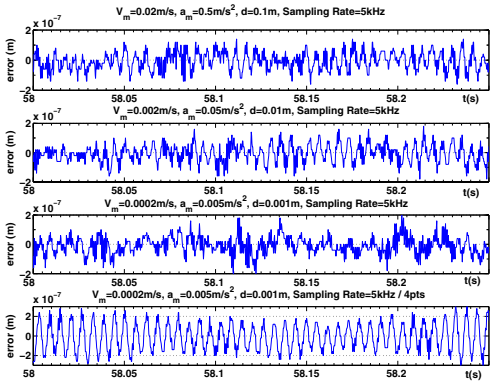

Fig. 9. Low Speed Experiments (Come to Stop Portion)

As a result, time-consuming and costly rigorous off-line identification of friction and ripple forces is avoided without sacrificing tracking performance. Comparative experimental results are obtained for the high-acceleration/high-speed as well as low-speed motion control of an iron core linear motor. The experimental results demonstrated that the proposed on-line cogging force compensation ARC controller not only maintain stability, but also deliver excellent tracking performance in all working conditions.

ACKNOWLEDGMENTS

The authors would like to thank Lv Lv, Wenjie Chen, and Zheng Chen for their help in obtaining the experimental results in the paper.

REFERENCES

[1] D. M. Alter and T. C. Tsao, "Control of linear motors for machine tool feed drives: design and implementation of h_∞ optimal feedback control," *ASME J. of Dynamic systems, Measurement, and Control*, vol. 118, pp. 649–656, 1996.

[2] B. Armstrong-Hélouvry, P. Dupont, and C. Canudas de Wit, "A survey of models, analysis tools and compensation methods for the control of machines with friction," *Automatica*, vol. 30, no. 7, pp. 1083–1138, 1994.

[3] P. V. Braembussche, J. Swevers, H. V. Brussel, and P. Vanherck, "Accurate Tracking control of Linear Synchronous Motor Machine tool Axes," *Mechatronics*, vol. 6, no. 5, pp. 507–521, 1996.

[4] T. Egami and T. Tsuchiya, "Disturbance Suppression Control with Preview Action of Linear DC Brushless Motor," *IEEE Transactions on Industrial Electronics*, vol. 42, no. 5, pp. 494–500, 1995.

[5] J. Y. Hung and Z. Ding, "Design of currents to reduce torque ripple in brushless permanent magnet motors," *Proc. Inst. Elect. Elect. Eng.*, vol. 140, no. 4, pp. 260–266, 1993.

[6] S. Komada, M. Ishida, K. Ohnishi, and T. Hori, "Disturbance Observer-Based Motion Control of Direct Drive Motors," *IEEE Transactions on Energy Conversion*, vol. 6, no. 3, pp. 553–559, 1991.

[7] G. Otten, T. Vries, J. Amerongen, A. Rankers, and E. Gaal, "Linear Motor Motion Control Using a Learning Feedforward Controller," *IEEE/ASME Transactions on Mechatronics*, vol. 2, no. 3, pp. 179–187, 1997.

[8] L. Xu and B. Yao, "Adaptive robust precision motion control of linear motors with ripple force compensation: Theory and experiments," in *Proc. of IEEE Conference on Control Applications*, Anchorage, 2000, pp. 373–378, (Winner of the Best Student Paper Competition).

[9] L. Xu and B. Yao, "Adaptive robust precision motion control of linear motors with negligible electrical dynamics: theory and experiments," *IEEE/ASME Transactions on Mechatronics*, vol. 6, no. 4, pp. 444–452, 2001.

[10] B. Yao, "High performance adaptive robust control of nonlinear systems: a general framework and new schemes," in *Proc. of IEEE Conference on Decision and Control*, San Diego, 1997, pp. 2489–2494.

[11] B. Yao, "Desired compensation adaptive robust control," in *Proceedings of the ASME Dynamic Systems and Control Division, DSC-Vol.64, IMECE'98*, Anaheim, 1998, pp. 569–575.

[12] B. Yao and M. Tomizuka, "Smooth robust adaptive sliding mode control of robot manipulators with guaranteed transient performance," *Trans. of ASME, Journal of Dynamic Systems, Measurement and Control*, vol. 118, no. 4, pp. 764–775, 1996, part of the paper also appeared in the *Proc. of 1994 American Control Conference*, pp.1176–1180.

[13] B. Yao and M. Tomizuka, "Adaptive robust control of SISO nonlinear systems in a semi-strict feedback form," *Automatica*, vol. 33, no. 5, pp. 893–900, 1997, (Part of the paper appeared in Proc. of 1995 American Control Conference, pp2500-2505, Seattle).

[14] B. Yao and L. Xu, "Adaptive robust control of linear motors for precision manufacturing," in *The 14th IFAC World Congress, Vol. A*, Beijing, 1999, pp. 25–30, the revised full version appeared in the *International Journal of Mechatronics*, Vol.12, No.4, pp595-616, 2002.

1-4244-1264-1/07/$25.00 ©2007 IEEE